

mTORC2 controls actin polymerization required for consolidation of long-term memory

Wei Huang^{1,2,7}, Ping Jun Zhu^{1,2,7}, Shixing Zhang^{3,4}, Hongyi Zhou^{1,2}, Loredana Stoica^{1,5}, Mauricio Galiano¹, Krešimir Krnjević⁶, Gregg Roman^{3,4} & Mauro Costa-Mattioli^{1,2,5}

A major goal of biomedical research is the identification of molecular and cellular mechanisms that underlie memory storage. Here we report a previously unknown signaling pathway that is necessary for the conversion from short- to long-term memory. The mammalian target of rapamycin (mTOR) complex 2 (mTORC2), which contains the regulatory protein Rictor (rapamycin-insensitive companion of mTOR), was discovered only recently and little is known about its function. We found that conditional deletion of *Rictor* in the postnatal murine forebrain greatly reduced mTORC2 activity and selectively impaired both long-term memory (LTM) and the late phase of hippocampal long-term potentiation (L-LTP). We also found a comparable impairment of LTM in dTORC2-deficient flies, highlighting the evolutionary conservation of this pathway. Actin polymerization was reduced in the hippocampus of mTORC2-deficient mice and its restoration rescued both L-LTP and LTM. Moreover, a compound that promoted mTORC2 activity converted early LTP into late LTP and enhanced LTM. Thus, mTORC2 could be a therapeutic target for the treatment of cognitive dysfunction.

How memories are stored in the brain is a question that has intrigued mankind over many generations. Neuroscientists have already made great strides in identifying key brain regions and relevant neuronal circuits, but many questions regarding the specialized molecular and neuronal mechanisms underlying memory formation remain unanswered. Post-translational modifications of synaptic proteins can explain transient changes in synaptic efficacy, such as short-term memory (STM) and the early phase of LTP (E-LTP, lasting 1–3 h), but new protein synthesis is required for long-lasting ones, such as LTM and L-LTP (lasting several hours)^{1–4}. Changes in actin dynamics that mediate structural changes at synapses are also necessary for L-LTP and for LTM storage^{5–7}. However, relatively little is known about the molecular mechanisms that underlie these processes.

The evolutionarily conserved mTOR forms two functionally distinct complexes^{8,9}. The first, mTORC1, consists of mTOR, Raptor and mLST8 (GβL), is sensitive to rapamycin and is thought to regulate mRNA translation rates^{3,10}. Although substantial progress has been made in the identification of the mTORC1 pathway and understanding its function in cells and *in vivo*, much less is known about the second complex, mTORC2. mTORC2 is largely insensitive to rapamycin and contains the core components mTOR, mSIN1, mLST8 and Rictor. Rictor is a defining component of mTORC2 and its interaction with mSIN1 appears to be required for mTORC2 stability and function¹¹. Rictor is associated with membranes and is thought to regulate the actin cytoskeleton, but the precise molecular mechanism behind this effect remains unclear^{8,9,11}. In addition, although little is known about mTORC2's upstream regulation, we are beginning

to understand its downstream regulation and effectors: mTORC2 phosphorylates AGC kinases at conserved motifs, including Akt at the hydrophobic motif site (Ser-473), the best characterized readout of mTORC2 activity^{8,9}.

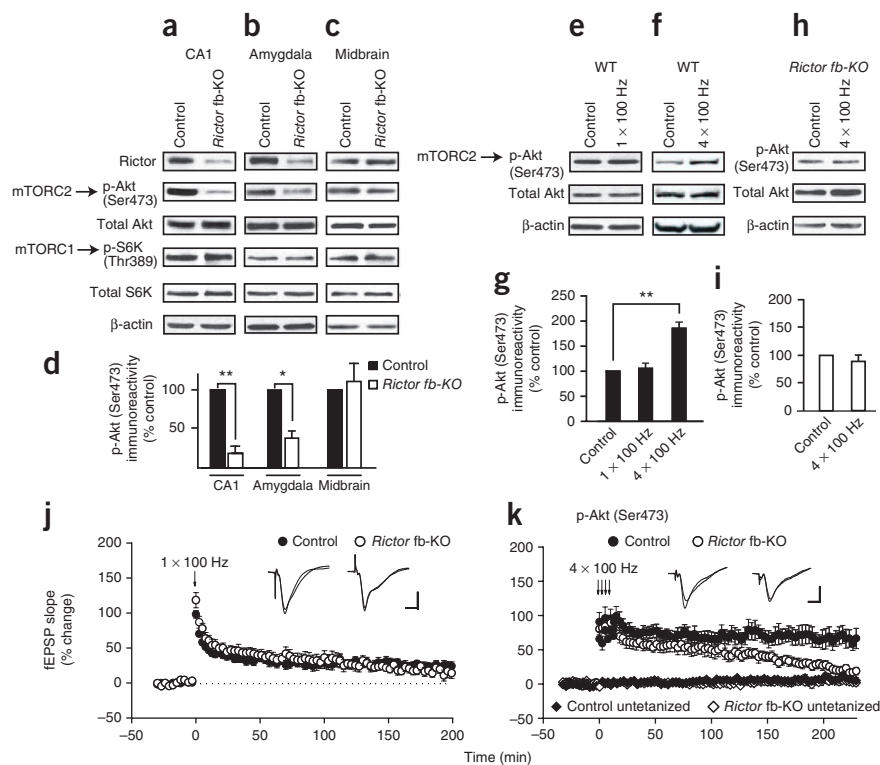
Rictor is important for embryonic development as mice lacking *Rictor* die in early embryogenesis^{12,13}. Rictor is highly expressed in the brain, notably in neurons¹³, and it seems to be crucial for various aspects of brain development and function. For example, genetic deletion of *Rictor* in developing neurons disrupts normal brain development, resulting in smaller brains and neurons, increased levels of monoamine transmitters, as well as manifestations of cerebral malfunction suggestive of schizophrenia and anxiety-like behaviors^{14,15}. In addition, mTORC2 signaling seems to be involved in mediating neuroadaptations to opiate drugs of abuse in ventral tegmental area dopaminergic neurons¹⁶.

Given that actin polymerization is critically required for memory consolidation^{5–7}, mTORC2 appears to regulate the actin cytoskeleton^{8,9}, and mTORC2's activity is altered in several cognitive disorders, including Huntington's disease, Parkinsonism, Alzheimer-type dementia and autism spectrum disorders^{17–21}, we decided to investigate its potential role in learning and memory formation, specifically in sustained changes in synaptic efficacy (LTP) in hippocampal slices and in behavioral tests of memory. We found that, through regulation of actin polymerization, mTORC2 is an essential component of memory consolidation. L-LTP and LTM were selectively impaired in mice and flies that were deficient for TORC2 signaling. Moreover, we identified the upstream synaptic events that activate mTORC2

¹Department of Neuroscience, Baylor College of Medicine, Houston, Texas, USA. ²Center on Addiction, Learning and Memory, Baylor College of Medicine, Houston, Texas, USA. ³Department of Biology and Biochemistry, University of Houston, Houston, Texas, USA. ⁴Biology of Behavior Institute, University of Houston, Houston, Texas, USA. ⁵Department of Molecular and Cell Biology, Baylor College of Medicine, Houston, Texas, USA. ⁶Department of Physiology, McGill University, Montreal, Canada. ⁷These authors contributed equally to this work. Correspondence should be addressed to M.C.-M. (costamat@bcm.edu).

Received 26 October 2012; accepted 29 January 2013; published online 3 March 2013; doi:10.1038/nn.3351

Figure 1 L-LTP, but not E-LTP, is impaired in mTORC2-deficient slices. **(a–c)** Western blots revealed a selective decrease in Rictor and mTORC2 activity (p-Akt Ser473) in CA1 **(a)** and amygdala **(b)**, but not in midbrain **(c)**, of *Rictor* fb-KO mice. **(d)** Normalized data (CA1, $n = 4$ per group, $t = 9.794$, $**P < 0.01$; amygdala, $n = 5$ per group, $t = 2.976$, $*P < 0.05$; midbrain, $n = 4$ per group, $t = 0.470$, $P = 0.663$). n values refer to the number of mice used, with one slice per mouse. **(e,f)** In CA1 extracts from wild-type mice, 30-min post-stimulation mTORC2 activity was consistently increased by four tetanic trains, but not by a single train. Hippocampal slices were stimulated at baseline frequency (0.033 Hz; control), tetanized by one train (100 Hz for 1 s; **e**), or four such trains at 5-min intervals (**f**). **(g)** Normalized mTORC2 activity ($n = 5$ per group; 1×100 Hz, $t = 0.31$, $P = 0.23$; 4×100 Hz, $t = 6.01$, $**P < 0.01$). **(h)** In CA1 from *Rictor* fb-KO mice, repeated trains failed to increase mTORC2 activity, as assayed 30 min post-stimulation. **(i)** Normalized data ($n = 5$ per group, $U = 5.00$, $P = 0.151$). **(j)** Similar E-LTP was elicited in control ($n = 9$) and *Rictor* fb-KO slices ($n = 8$) (LTP at 30 min: control, $41 \pm 5.6\%$; *Rictor* fb-KO, $44 \pm 5.7\%$; $F_{1,14} = 0.130$, $P = 0.724$; LTP at 180 min: controls, $23.7 \pm 5.3\%$; *Rictor* fb-KO, $24.7 \pm 8.5\%$; $F_{1,15} = 0.011$, $P = 0.917$). **(k)** L-LTP elicited by four trains in *Rictor* fb-KO slices ($n = 11$) was impaired versus control slices ($n = 14$; LTP was similar at 30 min, control $72 \pm 11.3\%$ and *Rictor* fb-KO $67 \pm 13.2\%$, $F_{1,23} = 0.811$, $P = 0.368$; at 220 min L-LTP was only $21 \pm 10.8\%$ for *Rictor* fb-KO slices versus $70 \pm 14.8\%$ for controls, $F_{1,23} = 23.4$, $P < 0.01$). Superimposed single traces were recorded before and 180 min after tetani (**j**) or before and 220 min after tetani (**k**). Scale bars represent 5 ms and 2 mV. All data are presented as mean \pm s.e.m. Full-length blots are shown in **Supplementary Figure 11**.



in the brain and the downstream molecular mechanism by which mTORC2 regulates L-LTP and LTM, namely regulation of actin polymerization. Finally, we found that a small molecule activator of mTORC2 and actin polymerization facilitated both L-LTP and LTM, further indicating that mTORC2 acts as a molecular switch for the consolidation of a short-term memory process into a long-term one.

RESULTS

Characterization of *Rictor* forebrain-specific knockout mice

Pharmacological inhibitors of mTORC2 are not available, and mice lacking *Rictor* in the developing brain show abnormal brain development^{14,15}. To circumvent this problem, we conditionally deleted *Rictor* in the postnatal forebrain by crossing mice in which *Rictor* is flanked by *loxP* sites¹³ with mice expressing Cre recombinase under the control of the α subunit of calcium/calmodulin-dependent protein kinase II (*Camk2a*) promoter²², generating *Rictor* forebrain-specific knockout mice (*Rictor*^{loxP/loxP}; *Camk2a-Cre*, *Rictor* fb-KO mice; see Online Methods and **Supplementary Fig. 1**). Because the *Camk2a* promoter is inactive before birth²³, this manipulation reduces the possibility of developmental defects caused by the loss of *Rictor*.

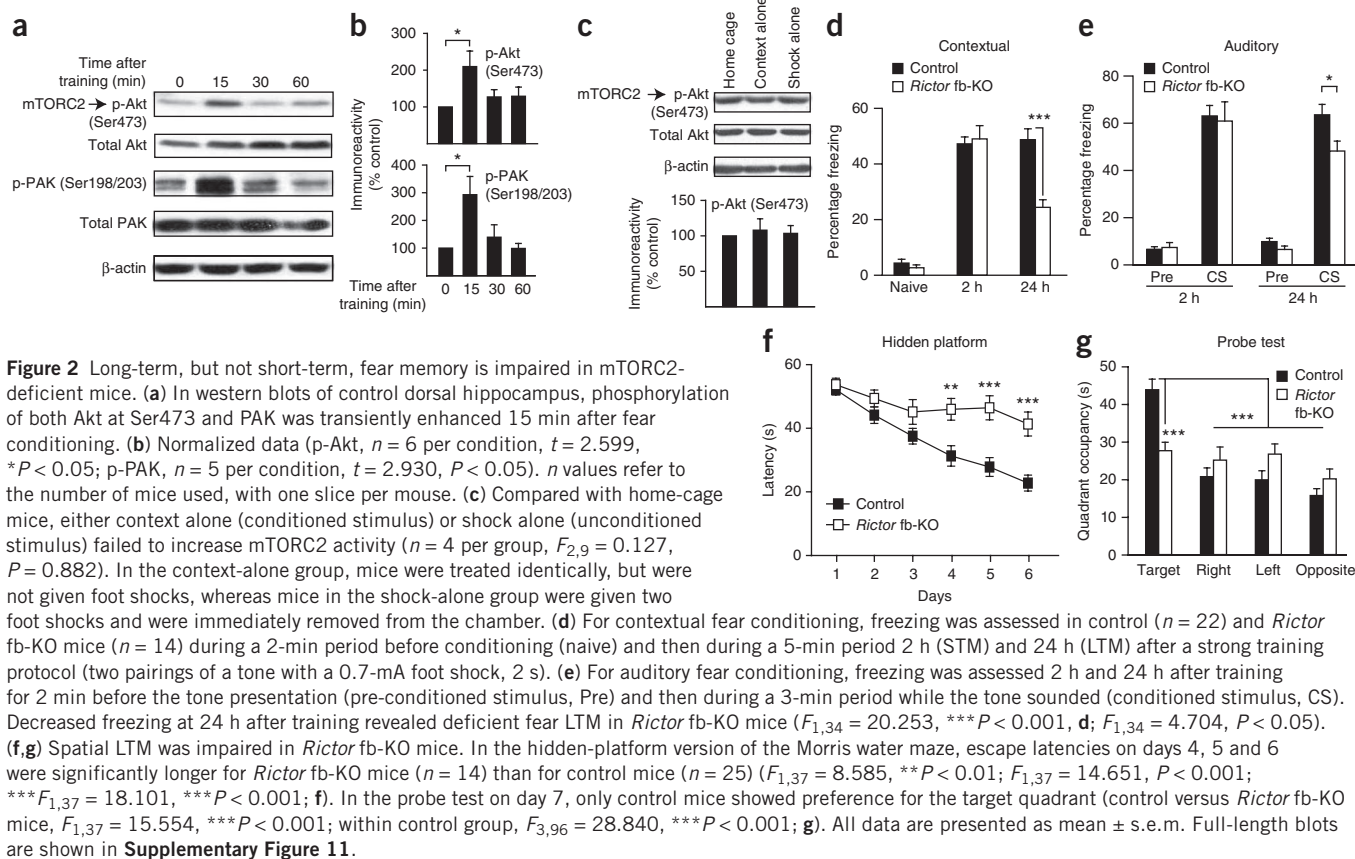
Rictor fb-KO mice were viable and developed normally. They showed neither gross brain abnormalities nor changes in the expression of several synaptic markers (**Supplementary Fig. 2**). mTORC2-mediated phosphorylation of Akt at Ser473 (an established readout of mTORC2 activity^{8,9}) was greatly reduced in CA1 and amygdala of *Rictor* fb-KO mice, but was normal in the midbrain (**Fig. 1a–d**). In contrast, in mTORC2-deficient mice, mTORC1-mediated phosphorylation of S6K1 at Thr389 (a well-established readout of mTORC1 activity¹⁰) remained unchanged in CA1,

amygdala or midbrain (**Fig. 1a–c**). Thus, conditional deletion of *Rictor* selectively reduces mTORC2 activity in forebrain neurons.

Deficient mTORC2 activity prevents L-LTP, but not E-LTP

To investigate the role of mTORC2 in synaptic function, we first examined whether triggers of synaptic plasticity, such as glutamate (via NMDA receptor, NMDAR) or neurotrophins, activate mTORC2. Indeed, we found that mTORC2 was activated in CA1 by either glutamate (100 μ M), NMDA (100 μ M) or brain-derived neurotrophic factor (BDNF, 50 ng ml⁻¹) (**Supplementary Fig. 3**), indicating that mTORC2 integrates information from various synaptic inputs. To determine whether short-term or long-term changes in synaptic potency alter mTORC2 activity, we compared the effects of one train of tetanic stimulation (100 Hz for 1 s), which usually induces only short-lasting E-LTP, with that of four such trains (which typically induce a long-lasting L-LTP)¹. Only the L-LTP-inducing stimulation consistently activated mTORC2 in CA1 neurons of control (**Fig. 1e–g**), but not *Rictor* fb-KO (**Fig. 1h,i**) mice. Hence, mTORC2 is selectively engaged in long-lasting synaptic changes in synaptic strength.

We then examined whether mTORC2 deficiency affects either E-LTP or L-LTP. A single train of tetanic stimulation generated a similar E-LTP in slices from *Rictor* fb-KO and control littermates (**Fig. 1j**), whereas four trains elicited a normal L-LTP in wild-type control slices, but not in *Rictor* fb-KO slices (**Fig. 1k**). Several tests revealed that the impaired L-LTP in mTORC2-deficient slices could not be attributed to defective basal synaptic transmission (**Supplementary Fig. 4**). Thus, reducing mTORC2 activity prevents the conversion of E-LTP into L-LTP.



Deficient TORC2 activity impairs LTM both in mice and flies

Given that L-LTP-inducing stimulation increases mTORC2 activity, we investigated whether mTORC2 is activated as a result of behavioral learning. Contextual fear conditioning, induced by pairing a context (conditioned stimulus) with a foot shock (unconditioned stimulus), resulted in a sharp temporary increase in mTORC2 activity and phosphorylation of the p21-activated kinase PAK (a regulator of actin cytoskeleton dynamics^{5–7}) 15 min after training (**Fig. 2a,b**). In contrast, the shock alone (unconditioned stimulus) and the context

alone (conditioned stimulus) failed to increase mTORC2 activity (**Fig. 2c**). Thus, hippocampal mTORC2 is selectively activated by behavioral learning (conditioned + unconditioned stimuli).

We then studied memory storage in two forms of Pavlovian learning: contextual and auditory fear conditioning. Contextual fear conditioning involves both the hippocampus and amygdala, whereas auditory fear conditioning, in which the foot shock (unconditioned stimulus) is paired with a tone (conditioned stimulus), requires only the amygdala²⁴. When mice were subsequently exposed to the same

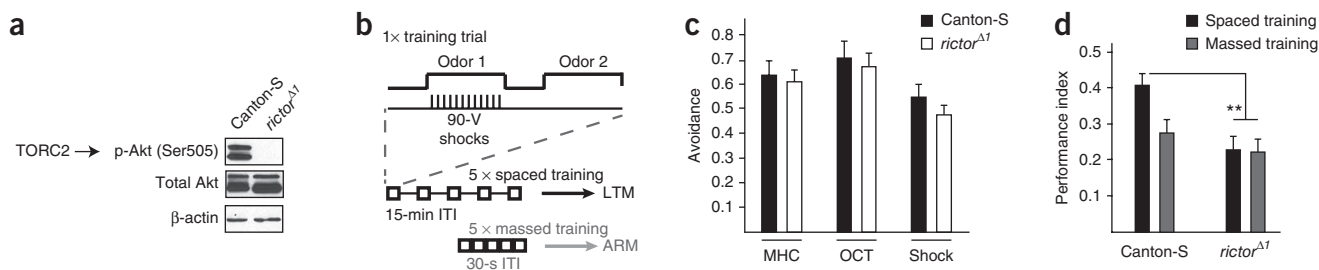
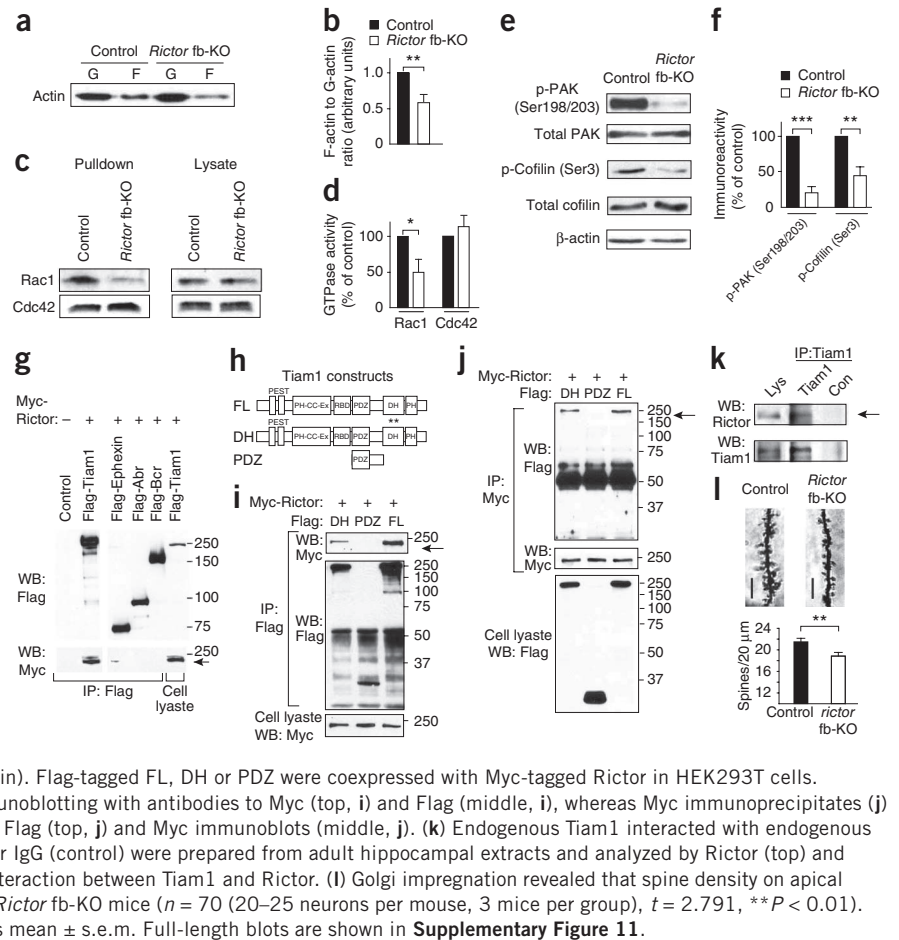


Figure 4 Actin dynamics, Rac1-GTPase activity and signaling are impaired in CA1 of *Rictor* fb-KO mice. (a–f) Western blotting revealed that the ratio of F-actin to G-actin (a), Rac1-GTPase (but not Cdc42) activities (c), and p-PAK and p-Cofilin expression (e) were much reduced in CA1 of *Rictor* fb-KO mice. Normalized data are shown in b, d and f (F-actin to G-actin ratio $n = 4$ per group, $t = 4.042$, $**P < 0.01$, b; Rac 1 activity, $n = 4$ per group, $t = 2.762$, $*P < 0.05$, d; Cdc42 activity, $n = 4$ per group, $t = 0.519$, $P = 0.623$, d; p-PAK $n = 4$ per group, $t = 9.054$, $***P < 0.001$, f; p-Cofilin $n = 4$ per group, $t = 4.486$, $**P < 0.01$, f). n values refer to the number of mice used, with one slice per mouse. (g) We hypothesized that mTORC2 regulates Rac1-GTPase activity (and signaling) through the recruitment of a specific Rac1-GTPase GEF. To test this hypothesis, we co-transfected HEK293T cells with Myc-tagged Rictor and Flag-tagged



co-immunoprecipitation (IP) experiments. Myc-Rictor selectively pulled down Flag-Tiam1. Flag-tagged Tiam1, ephexin, Abr and Bcr were coexpressed in HEK293T cells with Myc-Rictor and Flag immunoprecipitates were analyzed by antibodies to Flag (top) and Myc (middle). (h) Diagram of the Tiam1 constructs (FL = full length, DH = point mutations in the DH domain, PDZ = deletion mutant encoding only the PDZ domain). Flag-tagged FL, DH or PDZ were coexpressed with Myc-tagged Rictor in HEK293T cells. (i,j) Flag immunoprecipitates were analyzed by immunoblotting with antibodies to Myc (top, i) and Flag (middle, i), whereas Myc immunoprecipitates (j) were analyzed by immunoblotting with antibodies to Flag (top, j) and Myc immunoblots (middle, j). (k) Endogenous Tiam1 interacted with endogenous Rictor. Immunoprecipitates of antibodies to Tiam1 or IgG (control) were prepared from adult hippocampal extracts and analyzed by Rictor (top) and Tiam1 (bottom) immunoblots. Arrows point to the interaction between Tiam1 and Rictor. (l) Golgi impregnation revealed that spine density on apical dendrites of CA1 pyramidal neurons was reduced in *Rictor* fb-KO mice ($n = 70$ (20–25 neurons per mouse, 3 mice per group), $t = 2.791$, $**P < 0.01$). Scale bars represent 5 μ m. All data are presented as mean \pm s.e.m. Full-length blots are shown in **Supplementary Figure 11**.

conditioned stimulus, fear responses (freezing) were taken as an index of the strength of the conditioned stimulus–unconditioned stimulus association. *Rictor* fb-KO mice and control littermates showed similar freezing behavior before training (naive) and 2 h after training, when their STM was measured (Fig. 2d,e). However, when examined 24 h after training, both contextual and auditory LTM were impaired in mTORC2-deficient mice (Fig. 2d,e). The less pronounced change in auditory fear LTM versus contextual fear LTM in *Rictor* fb-KO mice may be explained by the smaller reduction in mTORC2 activity in the amygdala (Fig. 1a,b). Spatial LTM was also deficient in *Rictor* fb-KO mice when tested in the Morris water maze, where mice use visual cues to find a hidden platform in a circular pool²⁵. Compared with controls, *Rictor* fb-KO mice took longer to find the hidden platform (Fig. 2f), and they failed to remember the platform location in the probe test, performed on day 7 in the absence of the platform (target quadrant; Fig. 2g). The impaired spatial LTM was probably not caused by deficient visual or motor function, as control and *Rictor* fb-KO mice performed similarly when the platform was visible (Supplementary Fig. 5) and showed no difference in swimming speed (19.8 ± 0.6 versus 19.6 ± 0.5 cm s⁻¹ for control and *Rictor* fb-KO mice). Hence, mTORC2 selectively fosters long-term memory processes.

Because TORC2 is evolutionarily conserved^{8,9}, we also wondered whether its function in LTM formation is maintained across the animal phyla. To this end, we studied olfactory memory in wild-type controls (Canton-S) and *Drosophila* TORC2 (dTORC2)-deficient fruit flies. In the brain of *rictor* mutant flies (*rictor* ^{Δ})²⁶, dTORC2-mediated phosphorylation of the hydrophobic motif of Akt (Akt)

(an established readout of dTORC2 activity²⁷) was greatly reduced (Fig. 3a). As in mammals, LTM in *Drosophila* is protein synthesis dependent²⁸ and was generated after spaced training (five training sessions with a 15-min rest interval between each; Fig. 3b). In contrast, massed training (five training sessions with no rest intervals) failed to elicit LTM, but rather induced anesthesia-resistant, protein synthesis-independent memory (ARM; Fig. 3b)²⁸. Although responses to olfactory stimuli or electric shocks did not differ between *Rictor* ^{Δ} and control flies (Fig. 3c), LTM was blocked in *Rictor* ^{Δ} flies, whereas the short-lasting ARM was unaffected (Fig. 3d). Thus, TORC2 promotes LTM storage in both fruit flies and mice.

Deficient actin dynamics and signaling in mutant mice

We also probed the molecular mechanism by which mTORC2 regulates L-LTP and LTM by first testing whether mTORC2 deficiency impairs actin dynamics in CA1 neurons *in vivo*. Actin exists in two forms: monomeric globular actin (G-actin) and polymerized filamentous actin (F-actin), which is composed of aggregated G-actin. The transition between these two forms is controlled by synaptic activity⁵. The ratio of F-actin to G-actin, which reflects the balance between actin polymerization and depolymerization, was reduced in CA1 of *Rictor* fb-KO mice (Fig. 4a,b). Given that Rho-GTPases have been identified as important intracellular signaling molecules that regulate actin dynamics at synapses²⁹, we measured the activity of Rho-GTPases in CA1 of mTORC2-deficient mice. Rac1 (Ras-related C3 botulinum toxin substrate 1) and Cdc42 (cell division cycle 42), two Rho-GTPases, induce actin polymerization by promoting PAK and Cofilin phosphorylation⁵. Rac1 GTPase activity (but not

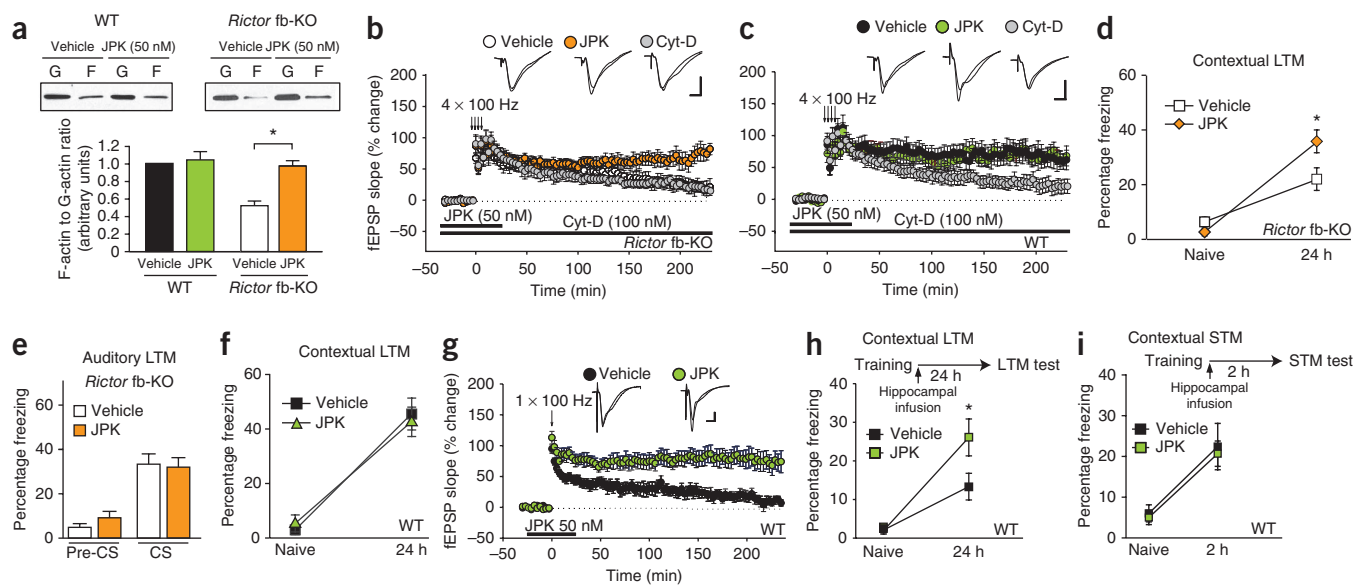


Figure 5 Restoring actin polymerization rescues the impaired L-LTP and contextual LTM caused by mTORC2 deficiency. (a) Western blots revealed that JPK (50 nM) increased the low F-actin to G-actin ratio in CA1 slices from *Rictor* fb-KO mice ($n = 4$ per group, $t = 3.821$, $*P < 0.05$), but not in control slices ($n = 4$ per group, $t = 0.253$, $P = 0.157$). n values refer to the number of mice used, with one slice per mouse. (b,c) The same concentration of JPK restored L-LTP in *Rictor* fb-KO slices ($n = 7$ per group, LTP at 30 min, vehicle = $67 \pm 7.7\%$, JPK = $73 \pm 11.3\%$, $H = 0.0667$, ANOVA on ranks, $P = 0.852$; LTP at 220 min, vehicle = $23 \pm 4.9\%$, JPK = $73 \pm 12.5\%$, $F_{1,12} = 9.81$, $P < 0.01$; b), but had no effect on L-LTP in wild-type slices ($n = 7$ per group, LTP at 30 min, vehicle = $74 \pm 9.4\%$, JPK = $72 \pm 11.4\%$, $F_{1,12} = 0.989$, $P = 0.784$; LTP at 220 min, vehicle = $64 \pm 8.7\%$, JPK = $68 \pm 14.2\%$, $F_{1,12} = 0.010$, $P = 0.921$; c). The actin polymerization inhibitor cytochalasin-D (Cyt-D, 100 nM) blocked L-LTP in wild-type slices (at 220 min, $26 \pm 7.8\%$, $F_{1,12} = 9.215$, $P < 0.01$; c), but had no effect in *Rictor* fb-KO slices (at 220 min, $21 \pm 7.9\%$, $F_{1,13} = 0.163$, $P = 0.694$; b). Insets in b and c are superimposed traces recorded before and 220 min after tetani. Scale bars represent 5 ms and 2 mV. (d,e) Bilateral infusion of JPK (50 ng) into the dorsal hippocampus of *Rictor* fb-KO mice ($n = 8$ per group) immediately after a strong training protocol (two pairings of a tone with a 0.7-mA foot shock, 2 s) boosted contextual LTM ($F_{1,14} = 4.827$, $*P < 0.05$; d), but not auditory LTM ($F_{1,14} = 0.0407$, $P = 0.843$; e). Freezing was assessed 24 h after training, as described in Figure 2. (f) In wild-type mice ($n = 8$ per group), JPK bilateral infusion (50 ng) had no effect on contextual LTM ($F_{1,14} = 0.129$, $P = 0.726$). (g) A single tetanic train elicited only E-LTP in vehicle-treated slices, but elicited a sustained L-LTP in JPK-treated slices ($n = 7$ for vehicle, $n = 8$ for JPK; LTP at 180 min, vehicle = $19 \pm 5.2\%$, JPK = $81 \pm 14.5\%$, ANOVA on ranks, $H = 10.59$, $P < 0.001$). Insets in g are superimposed single traces recorded before and 180 min after tetani. Scale bars represent 5 ms and 2 mV. (h,i) Intra-hippocampal infusion of JPK immediately after a weak training (a single pairing of a tone with a 1-s, 0.7-mA foot shock) enhanced contextual fear LTM, as assessed 24 h post-training ($n = 15$ for vehicle, $n = 16$ for JPK, $F_{1,29} = 4.320$, $*P < 0.05$, h), but not contextual fear STM, as assessed 2 h post-training ($n = 9$ for vehicle, $n = 10$ for JPK, $H = 0.00167$, ANOVA on ranks, $P = 0.967$, i). All data are presented as mean \pm s.e.m. Full-length blots are shown in Supplementary Figure 11.

Cdc42 activity) and the phosphorylation of PAK and Cofilin were greatly diminished in CA1 neurons of *Rictor* fb-KO mice (Fig. 4c–f). Moreover, we found that the Rac1-specific guanine nucleotide-exchange factor (GEF) Tiam1 (T-cell-lymphoma invasion and metastasis-1), which is highly enriched in neurons³⁰, linked Rictor (mTORC2) to Rac1 signaling (Fig. 4g–k). Finally, we found that dendritic spine density in CA1 pyramidal neurons was reduced in *Rictor* fb-KO mice (Fig. 4l). These data indicate that, in the adult hippocampus, mTORC2 regulates actin dynamics-mediated changes in synaptic potency and architecture via Rac1-GTPase signaling. However, we cannot rule out the possibility that the effects on actin polymerization are mediated by other mTORC2 targets, such as Akt or PKCalpha.

If L-LTP is impaired in mTORC2-deficient slices because actin polymerization is abnormally low, increasing the F-actin to G-actin ratio should convert the short-lasting LTP elicited by four tetanic trains into a normal L-LTP. We therefore predicted that jasplakinolide (JPK), a compound which directly promotes actin polymerization³¹, should restore normal function. Indeed, a low concentration of JPK (50 nM) raised the low F-actin to G-actin ratio and restored L-LTP in *Rictor* fb-KO slices (Fig. 5a,b), but had no effect on wild-type slices (Fig. 5a,c) or on baseline synaptic transmission in *Rictor* fb-KO slices (Supplementary Fig. 6a). In addition, cytochalasin D, an inhibitor

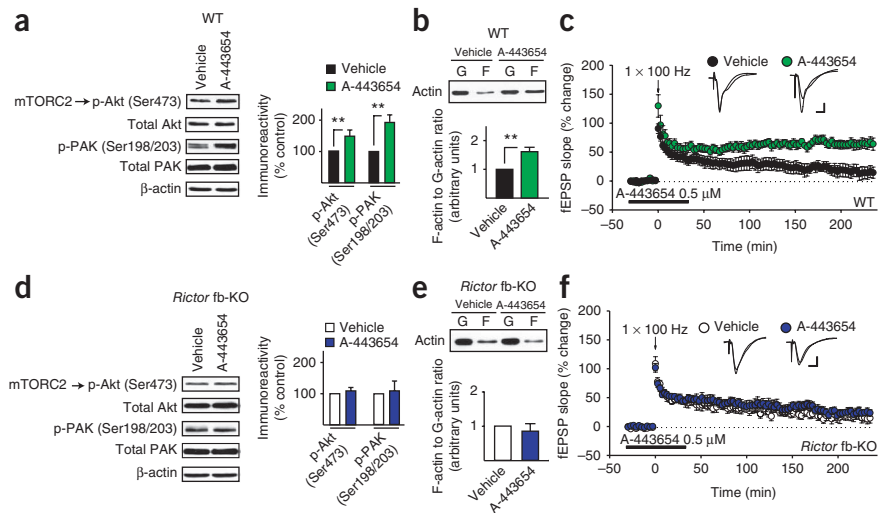
of actin polymerization, blocked L-LTP in wild-type slices (Fig. 5c), but had no effect on the short-lasting LTP evoked either by a single tetanic train in control slices (Supplementary Fig. 6b) or by repeated tetanic stimulation in mTORC2-deficient slices (Fig. 5b). The deficient L-LTP in mTORC2-deficient slices is therefore primarily caused by impaired actin polymerization.

To determine whether deficient actin dynamics underlie the impaired LTM in *Rictor* fb-KO mice, we bilaterally infused JPK into the CA1 region (Supplementary Fig. 7) at a low dose (50 ng) that promoted F-actin polymerization only in *Rictor* fb-KO mice (Supplementary Fig. 8a). JPK infused immediately after training boosted contextual LTM (Fig. 5d), but had no comparable effect on hippocampus-independent auditory LTM (Fig. 5e) in *Rictor* fb-KO mice or on contextual LTM in wild-type mice (Fig. 5f). These pharmacogenetic rescue experiments provide strong evidence that deficient actin dynamics account, at least in part, for the impaired LTM in *Rictor* fb-KO mice.

Stimulation of actin polymerization promotes L-LTP and LTM

Given that a short-lasting LTP is evoked by either repeated tetanic stimulation in mTORC2-deficient slices (Fig. 1k) or by a single tetanic train in control slices (Fig. 1j), and JPK restored the deficient L-LTP in mTORC2-deficient slices (Fig. 5b), we predicted that JPK would

Figure 6 A-443654 promotes mTORC2 activity, actin polymerization and facilitates L-LTP in wild-type mice, but not in mTORC2-deficient mice. **(a,b)** Treating wild-type hippocampal slices for 30 min with A-443654 (0.5 μ M) increased the activity of both mTORC2 and PAK ($n = 5$, $U = 0.00$, $**P < 0.01$; $n = 4$, $U = 0.00$, $P < 0.01$; **a**), as well as the F-actin to G-actin ratio ($n = 5$, $t = 3.995$, $P < 0.01$; **b**). n values refer to the number of mice used, with one slice per mouse. **(c)** A-443654 (0.5 μ M) converted E-LTP elicited by a single tetanic train into a sustained L-LTP in wild-type slices ($n = 6$ for vehicle, $n = 8$ for A-443654; LTP at 180 min, vehicle = $17 \pm 10.6\%$, A-443654 = $69 \pm 7.1\%$, $F_{1,12} = 17.870$, $P < 0.001$). **(d,e)** A-443654 (0.5 μ M) had no effect on mTORC2 and PAK activities ($n = 4$, $t = 0.830$, $P = 0.438$; $n = 4$, $t = 0.290$, $P = 0.777$; **d**) or on actin polymerization in *Rictor* fb-KO slices ($n = 3$, $t = 0.680$, $P = 0.534$; **e**). **(f)** A-443654 failed to convert E-LTP into L-LTP in *Rictor* fb-KO slices ($n = 6$ for vehicle, $n = 7$ for A-443654; LTP at 180 min, vehicle = $24 \pm 8.2\%$, A-443654 = $28 \pm 6.2\%$, $F_{1,11} = 2.25$, $P = 0.167$). Insets in **c** and **f** are superimposed traces recorded before and 180 min after tetani. Scale bars represent 5 ms and 2 mV. All data are presented as mean \pm s.e.m. Full-length blots are shown in **Supplementary Figure 11**.



facilitate the induction of L-LTP in control slices. Combining JPK with a weak stimulation, a single tetanus that normally elicits only a short-lasting E-LTP, we found that JPK lowered the threshold for the induction of L-LTP in wild-type slices (**Fig. 5g**).

Having found that boosting actin polymerization converts short-lasting LTP into long-lasting LTP, we next wondered whether this JPK-facilitated L-LTP depended on new protein synthesis. We found that the sustained L-LTP induced by a single train at 100 Hz in combination with JPK was blocked by the protein synthesis inhibitor anisomycin (**Supplementary Fig. 9a**). Furthermore, JPK could not rescue the impaired L-LTP induced by four trains at 100 Hz in the presence of anisomycin (**Supplementary Fig. 9b**). These data indicate that the actin cytoskeleton-mediated facilitation of L-LTP depends on protein synthesis.

We then bilaterally infused either JPK or vehicle into CA1 of wild-type mice immediately after a weak Pavlovian fear conditioning training (a single pairing of a tone with a 1-s, 0.7-mA foot shock). This protocol only generated a relatively weak memory in vehicle-infused mice, as measured 24 h after training (**Fig. 5h**). In contrast, in JPK-infused mice, the same protocol induced a greatly enhanced contextual fear LTM (**Fig. 5h**). As expected, JPK had no effect on contextual fear STM (**Fig. 5i**) or hippocampus-independent auditory fear LTM (**Supplementary Fig. 8b**). Because JPK acts directly on actin itself by increasing its polymerization³¹, these results support our hypothesis that actin polymerization is an essential mechanism for the consolidation of L-LTP and LTM.

Selective activation of mTORC2 enhances L-LTP and LTM

We then reasoned that direct activation of mTORC2 signaling should convert short-lasting to long-lasting memory processes (for both LTP and LTM). To test this hypothesis, we employed a small molecule (A-443654) that increases mTORC2-mediated phosphorylation of Akt at Ser473 (independently of mTORC1)³². We found that A-443654 promoted mTORC2 activity, PAK phosphorylation and actin polymerization in wild-type slices (**Fig. 6**), but not in mTORC2-deficient slices (**Fig. 6d,e**). Accordingly, A-443654 converted a short-lasting E-LTP into a sustained L-LTP in wild-type slices (**Fig. 6c**), but failed to do so in *Rictor* fb-KO slices (**Fig. 6f**). Thus, the facilitated L-LTP induced by combining A-443654 and a single high-frequency train is mediated by mTORC2.

If mTORC2 is involved in learning and memory formation, acute activation of mTORC2 should also promote LTM. Indeed, in wild-type mice, we found that an intraperitoneal injection of A-443654 increased the activity of both mTORC2 and PAK in the hippocampus (**Supplementary Fig. 10**). In addition, when wild-type mice were injected with either vehicle or A-443654 immediately after a weak Pavlovian fear conditioning training (a single pairing of a tone with a 1 s, 0.7 mA foot shock; **Fig. 7a**), we found that the A-443654-injected mice froze nearly twice as often as vehicle-injected controls 24 h later, indicating that their contextual LTM was enhanced (**Fig. 7b**). In contrast, A-443654 failed to enhance contextual LTM in mTORC2-deficient mice (**Fig. 7c**), confirming the selectivity of A-443654. A-443654 was injected post-training and contextual STM was not altered by A-443654 (**Fig. 7d**), arguing against nonspecific responses

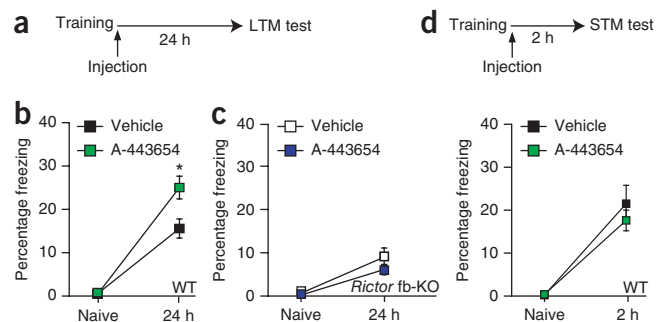


Figure 7 A-443654 selectively enhances LTM in wild-type mice, but not in mTORC2-deficient mice. **(a)** Diagram of the experimental protocol. **(b,c)** A single A-443654-injection (2.5 mg per kg of body weight intraperitoneal) immediately after a weak training (a single pairing of a tone with a 1-s, 0.7-mA foot shock) enhanced contextual fear LTM in wild-type mice ($n = 18$ per group, $F_{1,34} = 6.007$, $*P < 0.05$, **b**), but not in *Rictor* fb-KO mice ($n = 10$ per group, $F_{1,18} = 1.648$, $P = 0.22$, **c**). n values refer to the number of mice used, with one slice per mouse. **(d)** Similar freezing at 2 h reflects normal contextual fear STM in vehicle-injected and A-443654-injected wild-type mice ($n = 9$ for vehicle, $n = 10$ for A-443654, $F_{1,17} = 0.6$, $P = 0.449$). Freezing was assessed 2 h (**d**) or 24 h (**a-c**) after training, as described in **Figure 2**. All data are presented as mean \pm s.e.m. Full-length blots are shown in **Supplementary Figure 11**.

to fear. Taken together, these pharmacogenetic data suggest that A-443654's enhancing effect on synaptic plasticity and behavioral learning is dependent on mTORC2.

DISCUSSION

mTORC2 controls actin dynamics–dependent L-LTP and LTM

Although changes in synaptic actin dynamics are thought to occur during learning^{5–7}, the manner in which the synaptic actin cytoskeleton controls memory storage remains poorly understood. According to our findings, mTORC2 bidirectionally controls actin polymerization, which is required for the conversion of a short-term synaptic process (E-LTP and STM) into a long-lasting one (L-LTP and LTM). Specifically, we found that genetic inhibition of mTORC2 activity blocked actin polymerization and actin regulatory signaling (Fig. 4) and selectively suppressed LTM and L-LTP (Figs. 1 and 2). Conversely, activation of mTORC2 by A-443654 promoted actin polymerization and actin signaling and enhanced L-LTP and LTM in wild-type mice (Fig. 6a–c and Fig. 7a,b), but not in mTORC2-deficient mice (Fig. 6d–f and Fig. 7c).

Notably, pharmacologically restoring actin polymerization in mTORC2-deficient mice reversed the impairment of L-LTP and LTM (Fig. 5b,d). We speculate that the stabilization of the actin cytoskeleton in mTORC2-deficient neurons enables a morphological re-organization of the synapses, which, in response to activity, facilitates the trafficking and insertion of AMPA receptors clustered at the postsynaptic density. Consistent with this notion, spine density was reduced in mTORC2-deficient hippocampal neurons (Fig. 4l). Alternatively, the restoration of actin dynamics in mTORC2-deficient synapses could operate predominantly in a functional manner if the insertion of AMPA receptors occurs independently of changes in spine morphology³³. Another possibility is that actin remodeling could regulate changes in gene expression at synapses that are required for L-LTP and LTM (see below).

Other lines of evidence also support the hypothesis that mTORC2 promotes long-term changes in synaptic strength by promoting actin polymerization. First, L-LTP induction is associated with an increase in the F-actin to G-actin ratio^{34–36}, as well as with changes in synaptic morphology and actin signaling³⁷. Second, inhibitors of actin polymerization block L-LTP, leaving E-LTP intact^{38–40}. Consistent with these findings, only stimulation that induces a stable L-LTP reliably increases F-actin at spines³⁹. Third, direct activation of actin polymerization by JPK converted E-LTP into L-LTP and enhanced LTM (Fig. 5g,h). Fourth, the disruption of actin filaments in CA1 impairs the consolidation of contextual fear LTM⁴¹. Fifth, inhibition of actin polymerization and/or actin regulatory protein signaling in the lateral amygdala blocks auditory fear LTM but not STM^{42,43}. Finally, mTORC2 was activated during learning (Fig. 2a–c) and specifically by protocols that induced L-LTP (Fig. 1e–g).

Temporal and structural aspects of L-LTP and LTM

According to the prevailing view of memory consolidation, LTM is distinguished from STM by its dependence on protein synthesis^{1–4}. Consequently, all of the molecular switches identified so far are transcription or translation factors that regulate gene expression (from CREB⁴⁴ to eIF2 α ⁴⁵). However, similar to protein synthesis, mTORC2-mediated actin polymerization determines whether synaptic and memory processes remain transient or become consolidated in the brain. The evolutionary conservation of this new model, supported by our comparable findings in *Drosophila* (Fig. 3), also suggests that our findings may be relevant to the study of memory consolidation in higher mammals, including humans.

Whether actin-mediated changes in synaptic strength depend on, or are perhaps triggered by, changes in gene or protein expression is not immediately clear. An intriguing possibility is that changes in actin polymerization could directly affect changes in gene expression. For example, actin polymerization promotes the shuttling of the myocardin-related transcription factor MKL to the nucleus, where it interacts with the serum response factor, thus inducing activity-dependent gene expression in neurons⁴⁶. Another possibility is that the incorporation of G-actin into F-actin filaments could alter local translation at synapses by modulating the trafficking of ribosomes, translation initiation factors, RNA-binding proteins or even specific mRNAs⁴⁷. If so, the facilitated L-LTP induced by promoting actin polymerization should be insensitive to transcriptional inhibitors. In support of the idea that actin polymerization is upstream of protein synthesis, we found that the sustained L-LTP induced by a single train at 100 Hz in combination with JPK was blocked by anisomycin (Supplementary Fig. 9a). However, we cannot rule out the possibility that protein synthesis and actin polymerization occur in parallel during L-LTP and LTM.

Our results suggest that neurons have evolved a bimodal strategy that enables them to control L-LTP and LTM storage both temporally (through regulation of protein synthesis) and structurally (through control of actin dynamics). In this respect, given that mTOR regulates two important processes of L-LTP and LTM, mTORC1-mediated protein synthesis³ and mTORC2-mediated actin cytoskeleton dynamics, we propose that mTOR is an important regulator of memory consolidation, controlling distinct aspects: the temporal through mTORC1 and the structural through mTORC2.

Dysregulation of mTORC1 and mTORC2 signaling appears to have a crucial role in memory disorders, such as the cognitive deficit associated with autism spectrum disorder (ASD). Notably, the activity of mTORC2 is altered in the brain of ASD patients harboring mutations in *PTEN* and/or *TSC1* and *TSC2* (two upstream negative regulators of mTORC1)^{48,49}. In addition, in *PTEN* and *TSC2* ASD mouse models, prolonged rapamycin treatment *in vivo*, which indeed ameliorates the ASD-like phenotypes and restores mTORC1 activity, also corrects the abnormal mTORC2 activity^{20,50}. Our finding that mTORC2 is crucial for memory consolidation raises the possibility that the neurological dysfunction in ASD is caused by dysregulation of mTORC2 rather than by mTORC1 signaling. In conclusion, our results not only help to define basic cellular and molecular mechanisms of physiological learning and memory, but also point toward a new therapeutic approach for treating human memory dysfunction in cognitive disorders, in which mTORC2 activity is known to be abnormally low.

METHODS

Methods and any associated references are available in the [online version of the paper](#).

Note: Supplementary information is available in the online version of the paper.

ACKNOWLEDGMENTS

We thank M. Magnuson (Vanderbilt University), I. Dragatsis (University of Tennessee) and K. Tolias (Baylor College of Medicine) who generously provided *Rictor^{loxP/loxP}* mice, *Camk2a-Cre* mice and the Tiam1 constructs, respectively. We also thank A. Placzek and W. Sossin for comments on an early version of the manuscript. This work was supported by grants to M.C.-M. (National Institute of Mental Health grant MH 096816, National Institute of Neurological Disorders and Stroke grant NS 076708, Searle award grant 09-SSP-211, Whitehall award, grants from the George and Cynthia Mitchell Foundation) and G.R. (US National Institutes of Health grant MH091305 and a Texas Norman Hackerman Advanced Research Program award).

AUTHOR CONTRIBUTIONS

W.H., P.J.Z. and M.C.-M. conceived and designed the experiments. W.H. performed the behavioral, molecular and spine density experiments. P.J.Z. performed the electrophysiology experiments. H.Z. performed the Nissl staining experiments. G.R. and S.Z. performed and analyzed the *Drosophila* behavioral experiments. All of the authors discussed the results and commented on the manuscript. M.C.-M. wrote the manuscript with input from W.H., G.R., P.J.Z. and K.K.

COMPETING FINANCIAL INTERESTS

The authors declare no competing financial interests.

Reprints and permissions information is available online at <http://www.nature.com/reprints/index.html>.

- Kandel, E.R. The molecular biology of memory storage: a dialogue between genes and synapses. *Science* **294**, 1030–1038 (2001).
- McGaugh, J.L. Memory—a century of consolidation. *Science* **287**, 248–251 (2000).
- Costa-Mattioli, M., Sossin, W.S., Klann, E. & Sonenberg, N. Translational control of long-lasting synaptic plasticity and memory. *Neuron* **61**, 10–26 (2009).
- Wang, S.H. & Morris, R.G. Hippocampal-neocortical interactions in memory formation, consolidation and reconsolidation. *Annu. Rev. Psychol.* **61**, 49–79 C1–4 (2010).
- Cingolani, L.A. & Goda, Y. Actin in action: the interplay between the actin cytoskeleton and synaptic efficacy. *Nat. Rev. Neurosci.* **9**, 344–356 (2008).
- Lamprecht, R. & LeDoux, J. Structural plasticity and memory. *Nat. Rev. Neurosci.* **5**, 45–54 (2004).
- Lynch, G., Rex, C.S. & Gall, C.M. LTP consolidation: substrates, explanatory power and functional significance. *Neuropharmacology* **52**, 12–23 (2007).
- Guertin, D.A. & Sabatini, D.M. Defining the role of mTOR in cancer. *Cancer Cell* **12**, 9–22 (2007).
- Wullschlegel, S., Loewith, R. & Hall, M.N. TOR signaling in growth and metabolism. *Cell* **124**, 471–484 (2006).
- Ma, X.M. & Blenis, J. Molecular mechanisms of mTOR-mediated translational control. *Nat. Rev. Mol. Cell Biol.* **10**, 307–318 (2009).
- Oh, W.J. & Jacinto, E. mTOR complex 2 signaling and functions. *Cell Cycle* **10**, 2305–2316 (2011).
- Guertin, D.A. *et al.* Ablation in mice of the mTORC components raptor, rictor or mLST8 reveals that mTORC2 is required for signaling to Akt-FOXO and PKCalpha, but not S6K1. *Dev. Cell* **11**, 859–871 (2006).
- Shiota, C., Woo, J.T., Lindner, J., Shelton, K.D. & Magnuson, M.A. Multiallelic disruption of the rictor gene in mice reveals that mTOR complex 2 is essential for fetal growth and viability. *Dev. Cell* **11**, 583–589 (2006).
- Carson, R.P., Fu, C., Winzenburger, P. & Ess, K.C. Deletion of Rictor in neural progenitor cells reveals contributions of mTORC2 signaling to tuberous sclerosis complex. *Hum. Mol. Genet.* **22**, 140–152 (2013).
- Siuta, M.A. *et al.* Dysregulation of the norepinephrine transporter sustains cortical hypodopaminergia and schizophrenia-like behaviors in neuronal rictor null mice. *PLoS Biol.* **8**, e1000393 (2010).
- Mazei-Robison, M.S. *et al.* Role for mTOR signaling and neuronal activity in morphine-induced adaptations in ventral tegmental area dopamine neurons. *Neuron* **72**, 977–990 (2011).
- Griffin, R.J. *et al.* Activation of Akt/PKB, increased phosphorylation of Akt substrates and loss and altered distribution of Akt and PTEN are features of Alzheimer's disease pathology. *J. Neurochem.* **93**, 105–117 (2005).
- Humbert, S. *et al.* The IGF-1/Akt pathway is neuroprotective in Huntington's disease and involves Huntingtin phosphorylation by Akt. *Dev. Cell* **2**, 831–837 (2002).
- Malagelada, C., Jin, Z.H. & Greene, L.A. RTP801 is induced in Parkinson's disease and mediates neuron death by inhibiting Akt phosphorylation/activation. *J. Neurosci.* **28**, 14363–14371 (2008).
- Meikle, L. *et al.* Response of a neuronal model of tuberous sclerosis to mammalian target of rapamycin (mTOR) inhibitors: effects on mTORC1 and Akt signaling lead to improved survival and function. *J. Neurosci.* **28**, 5422–5432 (2008).
- Siarey, R.J. *et al.* Altered signaling pathways underlying abnormal hippocampal synaptic plasticity in the Ts65Dn mouse model of Down syndrome. *J. Neurochem.* **98**, 1266–1277 (2006).
- Dragatsis, I. & Zeitlin, S. CaMKIIalpha-Cre transgene expression and recombination patterns in the mouse brain. *Genesis* **26**, 133–135 (2000).
- Tsien, J.Z. *et al.* Subregion- and cell type-restricted gene knockout in mouse brain. *Cell* **87**, 1317–1326 (1996).
- LeDoux, J.E. Emotion circuits in the brain. *Annu. Rev. Neurosci.* **23**, 155–184 (2000).
- Morris, R.G., Garrud, P., Rawlins, J.N. & O'Keefe, J. Place navigation impaired in rats with hippocampal lesions. *Nature* **297**, 681–683 (1982).
- Hietakangas, V. & Cohen, S.M. Re-evaluating AKT regulation: role of TOR complex 2 in tissue growth. *Genes Dev.* **21**, 632–637 (2007).
- Sarbassov, D.D., Guertin, D.A., Ali, S.M. & Sabatini, D.M. Phosphorylation and regulation of Akt/PKB by the rictor-mTOR complex. *Science* **307**, 1098–1101 (2005).
- Tully, T., Preat, T., Boynton, S.C. & Del Vecchio, M. Genetic dissection of consolidated memory in *Drosophila*. *Cell* **79**, 35–47 (1994).
- Heasman, S.J. & Ridley, A.J. Mammalian Rho GTPases: new insights into their functions from *in vivo* studies. *Nat. Rev. Mol. Cell Biol.* **9**, 690–701 (2008).
- Tolias, K.F. *et al.* The Rac1-GEF Tiam1 couples the NMDA receptor to the activity-dependent development of dendritic arbors and spines. *Neuron* **45**, 525–538 (2005).
- Holzinger, A. Jaspalakinolide: an actin-specific reagent that promotes actin polymerization. *Methods Mol. Biol.* **586**, 71–87 (2009).
- Han, E.K. *et al.* Akt inhibitor A-443654 induces rapid Akt Ser-473 phosphorylation independent of mTORC1 inhibition. *Oncogene* **26**, 5655–5661 (2007).
- Kopec, C.D., Li, B., Wei, W., Boehm, J. & Malinow, R. Glutamate receptor exocytosis and spine enlargement during chemically induced long-term potentiation. *J. Neurosci.* **26**, 2000–2009 (2006).
- Fukazawa, Y. *et al.* Hippocampal LTP is accompanied by enhanced F-actin content within the dendritic spine that is essential for late LTP maintenance *in vivo*. *Neuron* **38**, 447–460 (2003).
- Matsuzaki, M., Honkura, N., Ellis-Davies, G.C. & Kasai, H. Structural basis of long-term potentiation in single dendritic spines. *Nature* **429**, 761–766 (2004).
- Okamoto, K., Nagai, T., Miyawaki, A. & Hayashi, Y. Rapid and persistent modulation of actin dynamics regulates postsynaptic reorganization underlying bidirectional plasticity. *Nat. Neurosci.* **7**, 1104–1112 (2004).
- Chen, L.Y., Rex, C.S., Casale, M.S., Gall, C.M. & Lynch, G. Changes in synaptic morphology accompany actin signaling during LTP. *J. Neurosci.* **27**, 5363–5372 (2007).
- Kim, C.H. & Lisman, J.E. A role of actin filament in synaptic transmission and long-term potentiation. *J. Neurosci.* **19**, 4314–4324 (1999).
- Kramár, E.A., Lin, B., Rex, C.S., Gall, C.M. & Lynch, G. Integrin-driven actin polymerization consolidates long-term potentiation. *Proc. Natl. Acad. Sci. USA* **103**, 5579–5584 (2006).
- Krucker, T., Siggins, G.R. & Halpain, S. Dynamic actin filaments are required for stable long-term potentiation (LTP) in area CA1 of the hippocampus. *Proc. Natl. Acad. Sci. USA* **97**, 6856–6861 (2000).
- Fischer, A., Sananbenesi, F., Schrick, C., Spiess, J. & Radulovic, J. Distinct roles of hippocampal *de novo* protein synthesis and actin rearrangement in extinction of contextual fear. *J. Neurosci.* **24**, 1962–1966 (2004).
- Lamprecht, R., Farb, C.R. & LeDoux, J.E. Fear memory formation involves p190 RhoGAP and ROCK proteins through a GRB2-mediated complex. *Neuron* **36**, 727–738 (2002).
- Mantzur, L., Joels, G. & Lamprecht, R. Actin polymerization in lateral amygdala is essential for fear memory formation. *Neurobiol. Learn. Mem.* **91**, 85–88 (2009).
- Bourtchuladze, R. *et al.* Deficient long-term memory in mice with a targeted mutation of the cAMP-responsive element-binding protein. *Cell* **79**, 59–68 (1994).
- Costa-Mattioli, M. *et al.* eIF2alpha phosphorylation bidirectionally regulates the switch from short- to long-term synaptic plasticity and memory. *Cell* **129**, 195–206 (2007).
- Olson, E.N. & Nordheim, A. Linking actin dynamics and gene transcription to drive cellular motile functions. *Nat. Rev. Mol. Cell Biol.* **11**, 353–365 (2010).
- Van Horck, F.P. & Holt, C.E. A cytoskeletal platform for local translation in axons. *Sci. Signal.* **1**, pe11 (2008).
- Choe, G. *et al.* Analysis of the phosphatidylinositol 3'-kinase signaling pathway in glioblastoma patients *in vivo*. *Cancer Res.* **63**, 2742–2746 (2003).
- Tsai, V. *et al.* Fetal brain mTOR signaling activation in tuberous sclerosis complex. *Cereb. Cortex* published online, doi:10.1093/cercor/bhs310 (18 October 2012).
- Zhou, J. *et al.* Pharmacological inhibition of mTORC1 suppresses anatomical, cellular and behavioral abnormalities in neural-specific Pten knock-out mice. *J. Neurosci.* **29**, 1773–1783 (2009).

ONLINE METHODS

Generation of *Rictor* fb-KO mice. *Rictor^{loxP/loxP}* mice¹³ were first backcrossed for eight generations with C57BL/6 mice and subsequently crossed with *Camk2a-Cre* mice (*Rictor^{+/+}; Camk2a-cre*)²². *Rictor^{loxP/loxP}; Camk2a-cre* mice were crossed to both *Rictor^{loxP/loxP}* mice and *Rictor^{loxP/loxP}* mice. We therefore studied the following experimental mice: *Rictor* fb-KO (*Rictor^{loxP/loxP}; Camk2a-cre* mice) and three sets of control littermates (*Rictor^{+/+}* mice, *Rictor^{+/+}; Camk2a-Cre* mice and *Rictor^{loxP/loxP}* mice). In our pilot LTP and behavioral experiments, there were no differences between these three control groups (Supplementary Fig. 1); the data from these three groups were pooled and defined as the control group (unless otherwise indicated). Mice were weaned at the third postnatal week and genotyped by PCR. *Rictor* mutant and wild-type alleles were detected by PCR assay in which primer PiaT41 (5'-ACTGAATATGTTTCATGGTTGTG-3') and primer PiaEx3 (5'-GAAGTTATTCAGATGGCCAGC-3') amplified a 466 base pair fragment (wild type) and a 554 base pair fragment (exon 3 of the *Rictor* conditional allele). Cre expression was detected by PCR with primers CreF2 (5'-GGCGTTTCTGAGCATACTGGAA-3') and CreR2 (5'-CACCATGCCCCGTTCACACTATC-3'), which amplify a 902 base pair fragment. All experiments were performed on 8–16-week-old males. The mice were kept on a 12-h light/dark cycle, and the behavioral tests were always conducted during the light phase of the cycle. The mice had access to food and water *ad libitum*, except during tests. Animal care and experimental procedures were approved by the animal care committee of Baylor College of Medicine, according to US National Institutes of Health Guidelines.

Electrophysiology. Horizontal hippocampal slices (350 μ m) were cut with a Leica (VT 1000S) vibratome from the brains of control or *Rictor* fb-KO littermates in 4 °C artificial cerebrospinal fluid (ACSF) and kept in ACSF at 22–24 °C for at least 1 h before recording^{51,52}. Slices were maintained in an interface-type chamber perfused (2–3 ml min⁻¹) with oxygenated ACSF (95% O₂ and 5% CO₂) containing 124 mM NaCl, 2.0 mM KCl, 1.3 mM MgSO₄, 2.5 mM CaCl₂, 1.2 mM KH₂PO₄, 25 mM NaHCO₃ and 10 mM glucose. Bipolar stimulating electrodes were placed in the CA1 stratum radiatum to excite Schaffer collateral and commissural fibers. Field excitatory postsynaptic potentials were recorded at 28–29 °C with ACSF-filled micropipettes. The recording electrodes were placed in the stratum radiatum and the intensity of the 0.1-ms pulses was adjusted to evoke 30–35% of maximal response. Tetanic LTP was induced by brief high-frequency trains (100 Hz, 1 s), applied either singly or in groups of four separated by 5-min intervals, as previously described^{51,52}. A stable baseline of responses at 0.033 Hz was established for at least 30 min. To reduce day-to-day variations, on a given day, we recorded from control and *Rictor* fb-KO slices or from slices treated with vehicle, JPK (Invitrogen), A-443654 (obtained from V. Giranda, Abbott Laboratories), cytochalasin-D (EMD Millipore) or anisomycin (Sigma). Furthermore, in a given experiment, we recorded from control and *Rictor* fb-KO slices in parallel from only one slice per genotype (in the same chamber to ensure uniformity in experimental conditions across groups). Thus, *n* values refer to both the number of slices and the number of mice.

Contextual and auditory fear conditioning. The experimenters were blind to the genotype and drug treatment for all behavioral tests. Fear conditioning was performed as previously described^{51,52}. Mice were first handled for 5 min for 3 d and then habituated to the conditioning chamber for 20 min for another day. On the training day, after 2 min in the conditioning chamber, mice received one pairing of a tone (2,800 Hz, 85 dB, 30 s) with a co-terminating foot shock (0.7 mA, 1 s) for the weak training protocol, or two pairings of a tone (2,800 Hz, 85 dB, 30 s) with a co-terminating foot shock (0.7 mA, 2 s) for the strong protocol, after which they remained in the chamber for an additional minute and were then returned to their home cages. At 2 h and 24 h after training, mice were tested for freezing (immobility with the exception of respiration) in response to the tone (in a chamber to which they had not been conditioned) and to the training context (training chamber).

During tests of auditory fear conditioning, mice were placed in the chamber and freezing responses were recorded during the initial 2 min (pre-conditioned stimulus period) and during the last 3 min when the tone sounded. Mice were returned to their cages 30 s after the end of the tone. For tests of contextual fear memory, mice were returned to the conditioning chamber for 5 min and freezing behavior was hand-scored at 5-s intervals by a rater who was blind to

the genotype. Tests of responses to the training context (chamber A) and to the tone (chamber B) were done in a counterbalanced manner. The percentage of time spent freezing was taken as an index of learning and memory. For the *in vivo* experiments, A-443654 was freshly dissolved in saline and then injected intraperitoneally at a dose of 2.5 mg per kg immediately after training.

Morris water maze. Tests were performed in a circular pool (140 cm of diameter) of opaque water (kept at 22–23 °C). *Rictor* fb-KO and control littermates were trained four times per day, at 30-min intertrial intervals, for 6 d as previously described⁴⁵. The latencies of escape from the water onto the hidden (submerged) platform (10 cm in diameter) were monitored by an automated video tracking system (HVS Image). For the probe trial, which was performed on day 7, the platform was removed from the pool and the mice were allowed to search for 60 s. The percentage of time spent in each quadrant of the pool (quadrant occupancy) was recorded. The mice were trained at the same time of day during their light phase.

Cannulation and JPK infusion. After intrahippocampal cannulation, mice were allowed a week to recover from surgery before the behavioral procedure. Briefly, mice were anesthetized with isoflurane (2–3%) and mounted in a stereotaxic frame. Bilateral cannulae (22 gauge), targeting the dorsal hippocampus, were implanted at an angle of 10° from the midline at these coordinates: anteroposterior = 2.0 mm, mediolateral = 1.8 mm, dorsoventral = 2.0 mm (as determined from a mouse brain atlas). Two jewelry screws were inserted into the skull and the cannulae were held in place by acrylic cement. A 28 gauge probe was inserted into the guide to prevent clogging. JPK (Invitrogen) was freshly dissolved in DMSO and further diluted in 0.9% NaCl (saline, wt/vol). We infused 1 μ l of JPK (50 ng) or vehicle bilaterally. The infusion was driven by a motorized syringe pump (KdScientific) at a rate of 0.2 μ l min⁻¹. Following 5 min of infusion the injector remained in the cannulae for an additional minute to allow complete diffusion of the solution from the tip of the injector. JPK was injected immediately after training and mice were trained as described above. After completion of the behavioral tests, mice were anesthetized with isoflurane and decapitated. The brains were fixed in 4% paraformaldehyde (wt/vol) and 50- μ m sections were cut and Nissl-stained to identify the placements of the cannulae. Only mice that had correct bilateral placements were included in the analyses. Cannulae and accessories were custom made by Plastic One.

Western blotting. Samples were homogenized in buffer containing 200 mM HEPES, 50 mM NaCl, 10% glycerol (vol/vol), 1% Triton X-100 (vol/vol), 1 mM EDTA, 50 mM NaF, 2 mM Na₃VO₄, 25 mM β -glycerophosphate and EDTA-free complete ULTRA tablets (Roche). A total of 50 μ g of protein per sample was resolved on SDS-PAGE (15%), transferred onto nitrocellulose membranes (Pall) and western blotting was performed as described earlier⁵¹.

Antibodies. For primary antibodies, we used antibodies to Rictor (#2140, 1:1,000), p-S6K1 (Thr389, #9234, 1:300), p-Akt (Ser473, #9271, 1:1,000), p-cofilin (Ser3, #3311, 1:1,000), total S6K (#9202, 1:1,000), total cofilin (#3312, 1:1,000), total Akt (#9272, 1:1,000), β -actin (#3700, 1:1,000), PSD95 (#2507, 1:1,000), synaptophysin (#4329, 1:1,000) and *Drosophila* p-Akt (Ser505, #4504, 1:1,000) (all from Cell Signaling and Technology Laboratories), GAD67 (MAB5406, 1:5,000, Millipore), p-PAK (Ser198/203) and total PAK (a generous gift from K. Tolias, Baylor College of Medicine)⁵³. Antibodies to Tiam1 (#sc-872), Myc (#sc-40) (both from Santa Cruz Biotech) and Flag (#F1804, Sigma) were used for immunoprecipitation.

F-actin to G-actin ratio. The F-actin to G-actin ratio was determined by western blotting, as previously described⁵⁴. Briefly, the two forms of actin differ in that F-actin is insoluble, whereas G-actin is soluble. The CA1 area of the hippocampus from control and *Rictor* fb-KO mice was isolated, homogenized in cold lysis buffer (10 mM K₂HPO₄, 100 mM NaF, 50 mM KCl, 2 mM MgCl₂, 1 mM EGTA, 0.2 mM DTT, 0.5% Triton X-100, 1 mM sucrose, pH 7.0) and centrifuged at 15,000g for 30 min. Soluble actin (G-actin) was measured in the supernatant. The insoluble F-actin in the pellet was resuspended in lysis buffer plus an equal volume of buffer 2 (1.5 mM guanidine hydrochloride, 1 mM sodium acetate, 1 mM CaCl₂, 1 mM ATP, 20 mM Tris-HCl, pH 7.5) and incubated on ice for 1 h to convert F-actin into soluble G-actin, with gentle mixing every 15 min. The samples were centrifuged at 15,000g for 30 min, and F-actin was measured

in this supernatant. Samples from the supernatant (G-actin) and pellet (F-actin) fractions were proportionally loaded and analyzed by western blotting using a specific actin antibody (#MAB1501, 1:10,000, Millipore).

Treatment of slices. *Ex vivo* slices treatment was carried out as previously described⁵¹. Slices were cut (350 μm) with a McIlwain Tissue Chopper (Mickle) and incubated for at least 1 h at 22–24 °C in oxygenated (95% O₂, 5% CO₂) ACSF before treatment. Slices were first treated with AP5 (100 μM), NBQX (100 μM), MK801 (50 μM), TrkB-Fc (1 $\mu\text{g ml}^{-1}$) or human IgG (1 $\mu\text{g ml}^{-1}$) for 30 min and then with glutamate (100 μM) or NMDA (100 μM) for 10 min or BDNF (50 ng ml⁻¹) for 30 min before snap-freezing over dry ice. In other slice recording experiments, slices were treated with JPK (50 nM) or A-443654 (0.5 μM). In all instances, slices were treated with vehicle as a control. Frozen slices were briefly thawed, and the CA1 area was microdissected, suspended in homogenizing buffer and analyzed by western blotting as described above.

Immunoprecipitations. *Myc-Rictor* cDNA was purchased from Addgene, whereas Flag-Tiam1, Flag-Abr, Flag-Bcr, Flag-ephexin, Flag-Tiam1-DH and Flag-Tiam1-PDZ were from K. Tolias (Baylor College of Medicine). HEK293T cells or hippocampal extracts were homogenized in ice-cold lysis buffer (40 mM HEPES (pH 7.5), 120 mM NaCl, 1 mM EDTA, 10 mM glycerophosphate, 50 mM NaF, 1.5 mM Na₃VO₃, 0.3% CHAPs (wt/vol) and EDTA-free complete ULTRA Tablets (Roche)). After centrifugation at 13,000g for 20 min, 2–5 μg of the indicated antibodies were added to the cleared supernatant and incubated with rotation for 1 h. Then, 30 μl of a 50% slurry of protein G-sepharose were added for 1 h (to the HEK293 extracts) or overnight (to the hippocampal extracts). Immunoprecipitates were washed four times with lysis buffer and samples were resolved by SDS-PAGE (10%) and immunoblotted with specific primary antibodies (as described above). The *n* values refer to both the number of slices and the number of mice.

Pull-down assays for Rac/Cdc42 GTPases. CA1 was dissected and homogenized in Mg²⁺ lysis buffer (Millipore) with complete protease inhibitor cocktail and assayed using Cdc42/Rac pull-down kit (#17-441, Millipore), according to the manufacturer's instructions. Briefly, samples were incubated with PAK-binding domain resin for 1 h at 4 °C. Beads were subsequently collected by centrifugation (10 s at 14,000g at 4 °C), washed and resuspended in Laemmli buffer. Western blotting was performed as described above using antibodies to Rac

(#05-389, 1:1,000, Millipore) or Cdc42 (#05-542, 1:1,000, Millipore). GTP and GDP loading controls were samples incubated with 100 μM GTP- γS or 1 mM GDP for 30 min at 30 °C.

Drosophila olfactory learning. The *Rictor*^{Δ1} flies²⁶ were out-crossed into a wild-type Canton-S background before behavioral experimentation. The negatively reinforced olfactory learning procedure was carried out according to established protocols^{28,55}, with some modifications. Briefly, the training odorants were 0.2% octanol (vol/vol, Sigma-Aldrich) and 0.12% methylcyclohexanol (vol/vol, Sigma-Aldrich) diluted in mineral oil. For each training trial, flies were exposed to the first odorant (CS⁺) and 12 1.25-s pulses of electric shock at 90 V for 1 min. This was followed by a 1-min presentation of the second odorant, which was not paired with shocks (CS⁻). Both spaced and massed training schedules had five training trials. The intertrial interval was 15 min for spaced training and 30 s for massed training. Memory was then tested in a T maze 24 h after the final training trial and the performance index calculated as: (number of flies that chose the CS⁻ – the number of flies that chose the CS⁺)/(total number of flies in both tubes), as previously described⁵⁵. Both octanol and methylcyclohexanol were used alternatively as the CS⁺, and the results were averaged for a single *n* value. For sensory controls, groups of flies were given 2 min to choose between odor and air or shocked and non-shocked side in a T maze. The odor concentrations and shock voltages were the same as in the LTM experiments.

Statistical analyses. All data are presented as means \pm s.e.m. The statistics were based on the Student's *t* test, one-way ANOVA and between-group comparisons using Tukey's test or ANOVA on ranks followed by Dunn's methods, unless otherwise indicated. *P* < 0.05 was considered significant.

51. Stoica, L. *et al.* Selective pharmacogenetic inhibition of mammalian target of Rapamycin complex I (mTORC1) blocks long-term synaptic plasticity and memory storage. *Proc. Natl. Acad. Sci. USA* **108**, 3791–3796 (2011).
52. Zhu, P.J. *et al.* Suppression of PKR promotes network excitability and enhanced cognition by interferon gamma-mediated disinhibition. *Cell* **147**, 1384–1396 (2011).
53. Shamah, S.M. *et al.* EphA receptors regulate growth cone dynamics through the novel guanine nucleotide exchange factor ephexin. *Cell* **105**, 233–244 (2001).
54. Zeng, L.H. *et al.* Kainate seizures cause acute dendritic injury and actin depolymerization *in vivo*. *J. Neurosci.* **27**, 11604–11613 (2007).
55. Ferris, J., Ge, H., Liu, L. & Roman, G. G(o) signaling is required for *Drosophila* associative learning. *Nat. Neurosci.* **9**, 1036–1040 (2006).